Proceedings of
The Fourth National Congress on Fluids Engineering
August 23-25, 2006, Kyungju, Korea

Prediction of Behavior for an Ultrasonically Driven Bubble in Sulfuric Acid Solutions by a Set of Solutions of Navier-Stokes Equations

Ki Young Kim*, Ki-Taek Byun** and Ho-Young Kwak***

나비아-스톡스 방정식의 해에 의한 황산용액 내에서 초음파에 의해 가진되는 기포의 거동 예측

김기영* · 변기택** · 곽호영***

Keywords : *Bubble (기포), Navier-Stokes Equations (나비아-스톡스 방정식), Sulfuric Acid Solutions (황산용액), Ultrasound (초음파)*

Abstract

A set of solutions of the Navier-Stokes equation for the gas inside a spherical bubble with heat transfer through the bubble wall permits to predict correctly behavior of an ultrasonically driven bubble in aqueous solutions of sulfuric acid. Calculation results of the minimum velocity of bubble wall and the peak temperature and pressure are in excellent agreement with the observed ones. Further the calculated bubble radius-time curve displays alternating pattern of bubble motion as observed in experiment.

1. 서 론

Bubble behavior under periodic pressure fields has drawn considerable attention because the subject is closely related to noise generation due to cavitation and to sonoluminescence [1, 2]. The dynamic behavior of bubbles, which might be described by the Rayleigh-Plesset (RP) equation [3] assuming incompressibility of liquid is a typical nonlinear phenomenon. Therefore, the response of a bubble, which is a nonlinear oscillator, to a periodic forcing field is difficult to predict the behavior.

In this study, the behavior of bubble oscillation under ultrasonic field in sulfuric acid solutions [4] was predicted by a set of solution of the Navier-Stockes equations for the gas inside bubble and a set of time dependent equations obtained from the Navier-Stokes equations for the liquid adjacent to the bubble wall [5].

2. Navier-Stokes Equation for the Gas inside Bubble and Liquid adjacent to the Bubble Wall

The hydrodynamics related to the behavior of bubbles in ultrasonic field involves in solving the Navier-Stokes equation for the gas inside bubble and the liquid adjacent to the bubble wall. The mass, momentum and energy equations for the gas inside the bubble with spherical symmetry are given as

$$\frac{\partial \rho_g}{\partial t}+\frac{1}{r^2}\frac{\partial}{\partial r}(\rho_g u_g r^2)=0, \tag{1}$$

$$\frac{\partial}{\partial t}(\rho_g u_g)+\frac{1}{r^2}\frac{\partial}{\partial r}(\rho_g u_g^2 r^2)+\frac{\partial P_b}{\partial r}=0, \tag{2}$$

$$\rho_g C_{v,b}\frac{DT_b}{Dt}=-\frac{P_b}{r^2}\frac{d}{dr}(r^2 u_g)-\frac{1}{r^2}\frac{d}{dr}(r^2 q_r), \tag{3}$$

A set of analytical solutions for the above conservation equations [5, 6] is given as

$$\rho=\rho_0+\rho_r \tag{4}$$

$$u_g=\frac{\dot{R}_b}{R_b}r, \tag{5}$$

$$P_b=P_{b0}-\frac{1}{2}\left(\rho_0+\frac{1}{2}\rho_r\right)\frac{\ddot{R}_b}{R_b}r^2, \tag{6}$$

$$T(r)=T_b(r)+T_b{}'(r) \tag{7}$$

where $\rho_g R_b^3=const.$ and $\rho_r=ar^2/R_b^5$. The constant a is related to the gas mass inside a bubble by $a/m=5(1-N_{BC})/4\pi$ with $N_{BC}=\left(P_{b0}R_b^3/T_{b0}\right)/\left(P_\infty R_0^3/T_\infty\right)$, where R_0 is the equilibrium bubble radius, and the subscript 0 denotes the properties at the bubble center. The linear velocity profile showing the spatial inhomogeneities inside the bubble is a crucial ansatz for the homologous motion of a spherical object, which is encountered in another energy focusing mechanism of gravitational collapse [7], and the quadratic pressure profile given in Eq. (4), was verified recently by comparisons with direct numerical simulations [8].

* 중앙대학교 대학원, kykim@wm.cau.ac.kr
** 중앙대학교 대학원, ctrlnew@wm.cau.ac.kr
*** 중앙대학교 기계공 kwakhy@cau.ac.kr

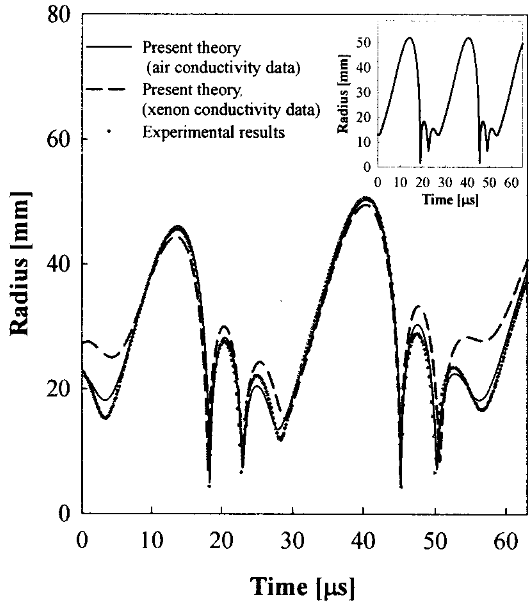

Figure. 1. Theoretical radius-time curve for xenon bubble of R_0=15.0μm at P_A=1.50 atm and f=37.8 kHz in sulfuric acid solution. The thermodynamic properties employed for 85 % sulfuric acid solution are ρ=1800 kg/m3, C_s=1470 m/s, μ=0.025 Ns/m2, σ=0.055 N/m, k_l=0.40 W/mK, and $C_{p,L}$=1,817 J/kgK.

The temperature profile due to the uniform pressure distribution $T_b(r)$ is well known and is perfectly valid for a nonsonoluminescing gas bubble [6]:

$$T_b(r)=\frac{B}{A}\cdot\left[-1+\sqrt{(1+\frac{A}{B}T_{bo})^2-2\eta\frac{A}{B}(T_{bl}-T_\infty)(\frac{r}{R_b})^2}\right], \tag{8}$$

where A and B are the are the coefficients in the temperature dependent gas conductivity having a form such as $k_g = AT+B$, $\eta=(R_b/\delta)/(k_l/B)$ and T_{bl} is the temperature at the bubble wall. For air $A=5.528\times10^{-5}$ J/msK^2 and $B=1.165\times10^{-2}$ J/msK and for xenon $A=1.0310\times10^{-5}$ J/msK^2 and $B=3.916\times10^{-3}$ J/msK were used. The temperature distribution due to the bubble wall acceleration, which is effective when the magnitude of the bubble wall acceleration exceeds $10^{12}m/s^2$ [5] is not considered in this study.

The mass and momentum equation for the liquid adjacent bubble wall provides the well-known equation of motion for the bubble wall [9], which is valid until the bubble wall velocity does not exceed the sound speed of the liquid. That is

$$R_b\left(1-\frac{U_b}{C_B}\right)\frac{dU_b}{dt}+\frac{3}{2}U_b^2\left(1-\frac{U_b}{3C_B}\right) \\ =\frac{1}{\rho_\infty}\left(1+\frac{U_b}{C_B}+\frac{R_b}{C_B}\frac{d}{dt}\right)\left[P_B-P_s\left(t+\frac{R_b}{C_B}\right)-P_\infty\right] \tag{9}$$

The liquid pressure on the external side of the bubble wall P_B is related to the pressure inside the bubble wall P_b by $P_B=P_b-2\sigma/R_b-4\mu U_b/R_b$. The pressure of the deriving sound field P_s may be represented by a sinusoidal function such as

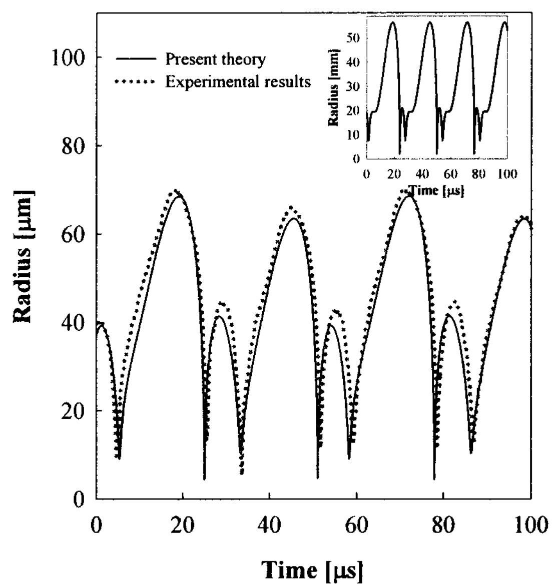

Figure 2. Theoretical radius time curve along with observed one for a xenon bubble of R_0=17.0μm at P_A=1.60 atm and f_d=37.8 kHz in sulfuric acid solution.

$P_s=-P_A\sin\omega t$ where $\omega=2\pi f_d$.

The mass and energy equation for the liquid provides a time dependent first order equation for the thermal boundary layer thickness δ with assumption of quadratic profile in temperature, which is given by [6]

$$\left[1+\frac{\delta}{R_b}+\frac{3}{10}\left(\frac{\delta}{R_b}\right)^2\right]\frac{d\delta}{dt}=\frac{6\alpha}{\delta}-\left[2\frac{\delta}{R_b}+\frac{1}{2}\left(\frac{\delta}{R_b}\right)^2\right]\frac{dR_b}{dt} \\ -\delta\left[1+\frac{1}{2}\frac{\delta}{R_b}+\frac{1}{10}\left(\frac{\delta}{R_b}\right)^2\right]\frac{1}{T_{bl}-T_\infty}\frac{dT_{bl}}{dt} \tag{10}$$

The above equation determines the heat flow rate through the bubble wall. Instantaneous bubble radius, bubble wall velocity and acceleration and the thermal boundary thickness obtained from Eqs. (9) and (10) provides density, velocity, pressure and temperature profiles for the gas inside the bubble without any further assumptions.

On the other hand, Hilgenfeldt et. al. [10] employed the "process equation" to obtained pressure inside a uniformly compressed bubble. The Rayleigh-Plesset equation with the so-called process equation will determine the bubble behavior in liquid under ultrasound. Certainly, the process equation which assumes the isothermal and uniform behavior of the gas inside bubble is not adequate to estimate the gas temperature inside the bubble. For calculating the temperature they employ a relation with variable polytropic indexes of γ which is related to the thermal diffusivity of gas and liquid and driving frequency [11]. Note that the uniform temperature approximation inside the bubble is valid when thermal equilibrium prevails.

3. Calculation Results and Discussion

The calculated radius-time curve for a xenon bubble with $R_0=15\mu m$, driven by the ultrasonic field with a frequency 37.8 kHz and amplitude of 1.5 atm in aqueous solution of sulfuric acid is shown in Fig. 1. With air data for the thermal conductivity, the calculated radius-time curve which exactly mimics the alternating pattern of the

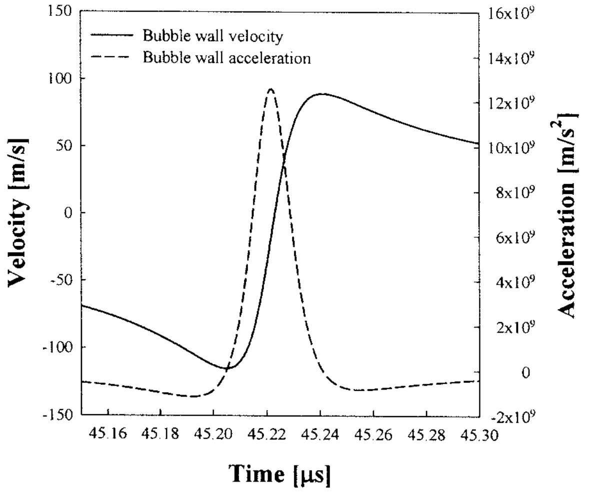

Figure 3. Calculated bubble wall velocity and acceleration near the collapse point for the bubble shown in Fig. 1.

observed result shows two different states of bubble motion. With xenon data, however, slight different pattern for the bubble motion was obtained. This happens due to the heat transfer across the bubble wall: more heat transfer in one cycle induces less minimum radius at the collapse point, which in turn produces larger maximum bubble radius in another cycle. Further, the added mass due to the increase in medium density and heat transfer through the bubble wall reduce the expansion ratio correspondingly they reduce the peak temperature, considerably. The calculated minimum bubble radius for the light-emitting cycles, $4.6\,\mu m$ is close to the observed value of $4.3\,\mu m$ [12]. As shown in Fig. 1 (insert), the calculated radius-time curve obtained by using the Higenfeldt et al.'s method does not show the alternating pattern.

Slight increase in the driving pressure amplitude yields quite different bubble radius-time curve. Figure 2 shows that bubble radius-time curve for a bubble with $R_0 = 17\,\mu m$ at $P_A = 1.6$ atm and $f_d = 37.8$ kHz. The calculated bubble radius-time curve also exactly mimics the observed one. Again, Higenfeldt et al.'s method does not yield correct bubble behavior as shown in the insert.

Figure 3 shows the time-dependent bubble wall velocity and the variation of the bubble wall acceleration around the collapse point for the bubble shown in Fig. 1. The calculated magnitude of the minimum velocity at the collapse point for the light emitting cycles is about $115\,m/s$ which is close to the observed velocity of $120\,m/s$. Whereas the maximum bubble wall velocity for non-light-emitting cycle is about $88\,m/s$, which is also close to the observed results of $80\,m/s$ [12]. The calculated maximum bubble wall acceleration is about $10^{10}\,m/s^2$. This value is smaller than the case of the sonoluminescing gas bubble in water by two orders of magnitude so that the gas pressure inside the bubble is almost uniform and the temperature increase due to the bubble wall acceleration is as small as 300K. However, the magnitude of the minimum velocity calculated by the Hilgenfeldt el al.'s method which is about $900\,m/s$ is much higher than the observed value.

Figure 4 shows the time dependent temperature calculated at the bubble center. The peak temperature calculated at the collapse point is about 8200 K, which is in excellent agreement with the observed value of 6000~7000 K. In fact, the average temperature at the collapse point is about 6000 K because considerable temperature drop occurs at the bubble wall as shown in Fig. 4 (insert). On the other hand, the pressure in the bubble is almost uniform as expected. Our calculated

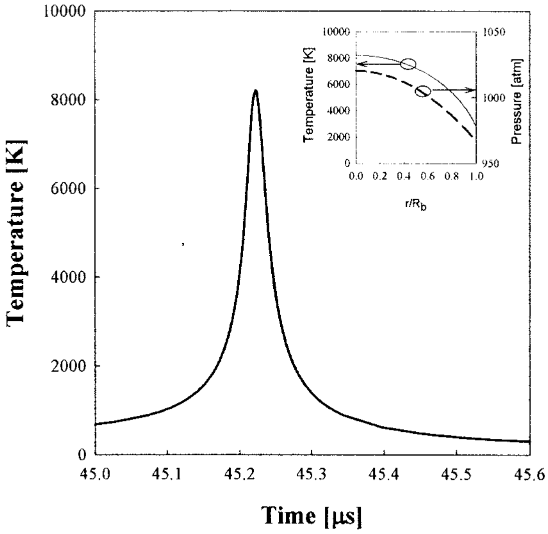

Figure 4. Time dependent gas temperature at the bubble center for the case shown in Fig. 1. The temperature and pressure distributions at the collapse point are shown in insert.

gas pressure at the collapse point for the argon bubble with $R_0 = 13\,\mu m$ driven at $P_A = 1.4$ bar and f_d=28.5 kHz in sulfuric acid solution is about 2800 atm, which is also close to the lower bound value of observed result, 1600 atm [13].

4. Conclusion

The behavior of ultrasonically driven bubble in sulfuric acid solutions has been found to be correctly predicted by a set of solution of the Navier-Stockes equations for the gas inside bubble with considering heat transfer through the bubble wall. The behavior of the bubbles turns out to depend crucially on the medium density and heat transfer through the bubble wall. The calculated bubble radius-time curve which mimics the observed one shows alternating pattern of bubble motion.

Acknowledgement

This work has been supported by a grant from Electric Power Research Institute(EPRI) in the USA, under contract EP-P19394/C9578.

References

[1] Gaitan, D. F., Crum, L. A., Church, C. C., and Roy, R. A., 1992, "Sonoluminescence and Bubble Dynamics for a Single, Stable, Cavitation Bubble," Journal of Acoustical Society of America, Vol 91, pp. 3166-3183.

[2] Putterman, S. J. and Weninger, K. R., 2000, Sonoluminescence : How Bubble Turn Sound into Light, Annu. Rev. Fluid Mech. 32, 445-476.

[3] Young, F. R., 1989, Cavitation, MaGraw-Hill.

[4] Flannigan, D. J. and Suslick, K. S., 2005, "Plasma Formation and Temperature Measurement during Single-Bubble Cavitation," Nature, Vol. 434, pp. 52-55.

[5] Kwak, H. and Na, J., 1996, "Hydrodynamic Solutions for a Sonoluminescing Gas Bubble," Physical Review Letter, Vol. 77, pp. 4454-4457.

[6] Kwak, H. and Yang, H., 1995, "An Aspect of Sonoluminescence

from Hydrodynamic Theory," Journal of Physical Society of Japan, Vol. 64, pp. 1980-1992.
[7] Jun, J. and Kwak, H., 2000, "Gravitational Collapse of Newtonian Star," International Journal of Modern Physics D, Vol. 9, pp. 35-42.
[8] Lin, H., Storey, B. D., and Szeri, A. J., 2002, "Inertially driven inhomogeneities in Violently Collapsing Bubbles: the Validity of the Rayleigh-Plesset Equation," Journal of Fluid Mechanics, Vol. 452, pp. 145-162.
[9] Keller, J. B. and Miksis, M., 1980, "Bubble Oscillations of Large Amplitude," Journal of Acoustical Society of America, Vol. 68, pp. 628-633.
[10] Hilgenfeldt, S., Lohse, D., and Brenner, M. P., 1996, Phase Diagrams for Sonoluminescing in Bubbles, Physics of Fluids Vol., Vol. 8, pp. 2808-2826.
[11] Prosperetti, A., Crum, L. A., and Commander, K. W., 1998, "Nonlinear Bubble Dynamics," Journal of Acoustical Society of America, Vol. 83, pp. 502-514.
[12] Hopkins, S. D., Putterman, S. J., Kappus, B. A., Suslick, K. S., and Camara, C. G., 2005, "Dynamics of a Sonoluminescing Bubble in Sulfuric Acid," Physical Review Letter, Vol. 95, pp. 254301.
[13] Flannigan, D. J., Hopkins, S. D., Camara, C. G., Putterman, S. J., and Suslick, K. S., 2006, "Measurement of Pressure and Density Inside a Single Sonoluminescing Bubble", Physical Review Letter, Vol. 96, pp. 204301.